AGU PUBLICATIONS

Geophysical Research Letters

RESEARCH LETTER
10.1002/2013GL058799

Key Points:
- Carbon export to 1000 m does not guarantee sequestration in the Southern Ocean
- OIF requires consideration of the circulation as well as biogeochemistry
- Sequestered carbon is dispersed widely out of the Southern Ocean by circulation

Supporting Information:
- Readme
- Table S1
- Table S2
- Table S3
- Table S4
- Movie S1
- Movie S2
- Figure S1

Correspondence to:
J. Robinson,
josie.robinson@noc.soton.ac.uk

Citation:
Robinson, J., E. E. Popova, A. Yool, M. Srokosz, R. S. Lampitt, and J. R. Blundell (2014), How deep is deep enough? Ocean iron fertilization and carbon sequestration in the Southern Ocean, *Geophys. Res. Lett.*, *41*, 2489–2495, doi:10.1002/2013GL058799.

Received 10 JAN 2014
Accepted 20 MAR 2014
Accepted article online 25 MAR 2014
Published online 11 APR 2014

How deep is deep enough? Ocean iron fertilization and carbon sequestration in the Southern Ocean

J. Robinson[1,2], E. E. Popova[2], A. Yool[2], M. Srokosz[2], R. S. Lampitt[2], and J. R. Blundell[1]

[1]Ocean and Earth Science, University of Southampton, Southampton, UK, [2]National Oceanography Centre, Southampton, UK

Abstract Artificial ocean iron fertilization (OIF) enhances phytoplankton productivity and is being explored as a means of sequestering anthropogenic carbon within the deep ocean. To be considered successful, carbon should be exported from the surface ocean and isolated from the atmosphere for an extended period (e.g., the Intergovernmental Panel on Climate Change's standard 100 year time horizon). This study assesses the impact of deep circulation on carbon sequestered by OIF in the Southern Ocean, a high-nutrient low-chlorophyll region known to be iron stressed. A Lagrangian particle-tracking approach is employed to analyze water mass trajectories over a 100 year simulation. By the end of the experiment, for a sequestration depth of 1000 m, 66% of the carbon had been reexposed to the atmosphere, taking an average of 37.8 years. Upwelling occurs predominately within the Antarctic Circumpolar Current due to Ekman suction and topography. These results emphasize that successful OIF is dependent on the physical circulation, as well as the biogeochemistry.

1. Introduction

The Intergovernmental Panel on Climate Change Fifth Assessment Report (IPCC AR5) states that the climate has and is warming, unequivocally, and we can now be 95–100% certain that since the midtwentieth century, it is primarily due to anthropogenic influence [*Intergovernmental Panel on Climate Change (IPCC), Working Group I (WGI)*, 2013]. Against this backdrop of increasing greenhouse gas emissions and global climate change, a number of schemes have been proposed to "geoengineer" the Earth's climate. Ocean iron fertilization (OIF) is one such scheme aimed at modifying the biogeochemical cycle of carbon in the ocean in order to increase the oceanic uptake of CO_2. OIF is intended to artificially stimulate the biological pump by exploiting the surplus macronutrients found in so-called high-nutrient low-chlorophyll (HNLC) regions where biological activity is restricted by the availability of the micronutrient iron [*Martin*, 1990]. The Southern Ocean (SO) is by far the largest expanse of HNLC waters and is iron stressed because overlying air masses circle the Earth in a latitude band that has sparse landmass and thus supplies little iron-rich aeolian dust. Consequently, the SO has been identified as a particularly favorable location for OIF [*Lampitt et al.*, 2008].

In the Intergovernmental Panel on Climate Change Fourth Assessment Report (IPCC AR4) successful iron fertilization is divided into phases, of which artificial stimulation of a surface phytoplankton bloom is only the first. For the second phase, a proportion of the particulate organic carbon (POC) produced must sink down the water column and reach the main thermocline or deeper before being remineralized. Finally, the third phase is long-term sequestration of the carbon at depth out of contact with the atmosphere. Characterizing the relevant time and space scales for sequestration is not a wholly objective procedure [*Leinen*, 2008]. Nonetheless, the 100 year time scale adopted in IPCC forecasting is frequently used [*Oschlies et al.*, 2010; *Rickels et al.*, 2010], and the typical depth of the main thermocline, 1000 m [*IPCC, WGI*, 2007, chapter 5], serves as a vertical horizon clearly removed from the surface ocean and atmosphere [*Passow and Carlson*, 2012].

Here we investigate these spatiotemporal scales, specifically the long-term fate of carbon that reaches the deep ocean. Model simulations of the trajectories of Lagrangian particles associated with geoengineered carbon are performed to establish the fate of such material. Statistical analysis of the resulting deep ocean pathways is then used to evaluate carbon sequestration in the SO, with a particular focus on the significance of the 1000 m depth horizon and centennial time scale.

2. Methodology

The Nucleus for European Modelling of the Ocean (NEMO) model is an ocean general circulation model (GCM). The NEMO 1/4° resolution model has been developed with particular emphasis on realistic representation of fine-scale circulation patterns [*Madec*, 2008] and provides an ideal platform to conduct Lagrangian particle-tracking experiments. Here we use 10 years of monthly averaged circulation output from 1997 to 2006 that we cycle 10 times to create a 100 year simulation. The Ariane package [*Blanke and Raynaud*, 1997] (available online at: http://stockage.univ-brest.fr/~grima/Ariane) is applied to the resulting 100 year NEMO velocity field to track water parcels using point particles that are released into the modeled ocean circulation [*Popova et al.*, 2013]. These particles are intended here to represent water masses within which sinking POC, produced through the activities of surface OIF, has been remineralized to dissolved inorganic carbon. They should not be confused with actual POC particles, since their modeled behavior (neutral buoyancy and indefinite lifespan) does not emulate that of sinking biogenic material.

To test the suitability of the 1000 m minimum depth recommendation by the IPCC AR4 [*IPCC WGI*, 2007, chapter 5; *IPCC WGIII*, 2007, chapter 11] for OIF, we deploy Lagrangian particles across the SO at a depth of 1000 m. Particles are placed south of the midpoint between the nitrate maxima to the south and nitrate-depleted waters to the north, which represents the northern limit of the HNLC region in the SO. The particles are spaced regularly across the model grid, and, accounting for bathymetric features shallower than 1000 m, this gives a total of 24982 particles, a sufficient number to resolve SO water mass pathways. During the 100 year simulation, particle trajectories (horizontal position and depth) are recorded at monthly intervals.

The upper mixed layer (UML) of the ocean is characterized by vigorous mixing and near-homogeneous physical and biogeochemical properties and represents the volume of water in close contact with the atmosphere [*Sprintall and Cronin*, 2009]. Here we use the base of the UML, referred to as the mixed layer depth (MLD), as the key boundary to separate failed and successful carbon sequestration, judging any Lagrangian trajectories that enter the UML as potential pathways for OIF carbon to escape back in to the atmosphere. In our analysis we specifically define our boundary, MLDX, as the modeled (local) mean annual maximum MLD rather than instantaneous MLD. The advantage of this approach is that it uses a single horizon to determine leakage of OIF carbon, however, a sensitivity analysis was performed using the maximum annual maximum depth of the MLD and also the actual monthly MLD which only minimally altered the results.

The accuracy of the model-derived MLD was examined by comparison with the MLD calculated from World Ocean Atlas (WOA) 2009 fields of temperature [*Locarnini et al.*, 2010] and salinity [*Antonov et al.*, 2010], using two criteria: a density change of 0.125 (sigma units) and a variable density change corresponding to a temperature change of 0.5°C [*Monterey and Levitus*, 1997], both calculated 10 m from the surface to avoid complications with ice cover. Repeating our central analysis using an observation-derived MLDX, we found that the difference between using the WOA- and NEMO-calculated MLDX to be relatively small. Therefore, and since it is consistent with NEMO's velocity field, we refer only to the NEMO-derived MLDX in the rest of this paper, which was determined using the density calculation method with a critical value of 0.01 (sigma units). Full details on the MLDX sensitivity analysis and comparison with observations, including the global and SO mean MLD, can be found in Tables S1 and S2 in the supporting information. Additionally, Figure S1 in the supporting information shows the NEMO-derived mean annual maximum MLD that is used in the analysis, MLDX, referred to as *NEMO Diagnostic (Sigma, 0.01)* in Table S2.

3. Results

Of the 24982 Lagrangian particles that were injected into the SO at 1000 m, 66% were advected above MLDX taking an average of 37.8 (σ = 22.2) years. In Figure 1 each marker represents the location where a particle crossed the MLDX boundary, with the color indicating the time in years. The most significant feature of Figure 1 is the large-scale sequestration failure within the SO, which accounts for the majority (97%) of all leakage into the UML (average: 37.4 (σ = 22.2) years to fail). The particle advection into the UML can be attributed to the Antarctic Circumpolar Current (ACC), which circulates Antarctica in an eastward direction [*Rintoul*, 2011]. Lagrangian particles caught in the ACC are transported across MLDX as the current is forced up and over sea floor topography, predominately the Scotia Ridge Arc System and the Kerguelen Plateau. The deep dense water (containing the particles at 1000 m) is mixed with the overlying lighter water mass, gaining buoyancy and gradually transporting the particles above MLDX. In addition to advection into the

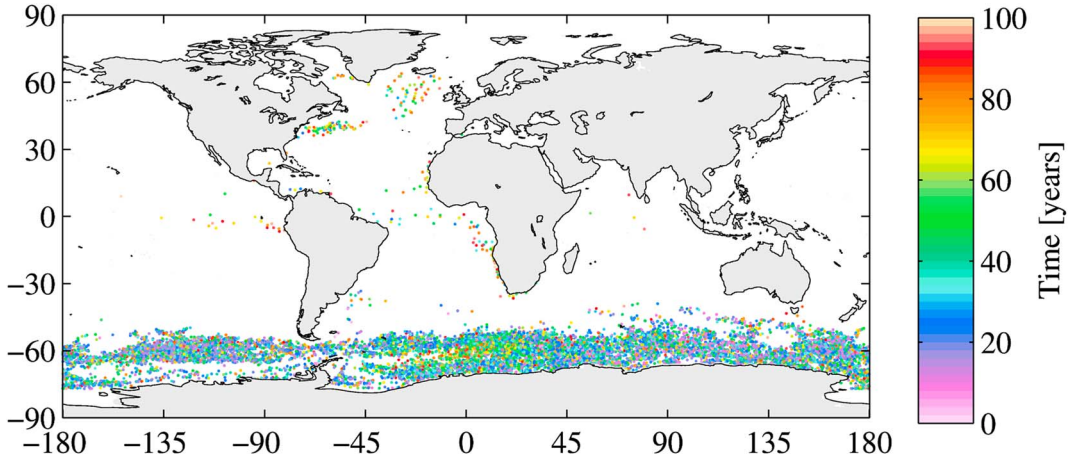

Figure 1. Colored markers represent locations where the Lagrangian particles enter the upper mixed layer. The color of a marker represents the time (years) it took to reach the upper mixed layer within the 100 year run.

UML, there is also Ekman suction occurring in the SO, which upwells the particles south of the Westerlies wind stress maximum over the axis of the ACC [*Sarmiento and Gruber*, 2006]. This is particularly visible in the Pacific and Atlantic sectors of Figure 1, between the latitude bands of 55°S–65°S.

The SO has a particularly energetic circulation connecting the three major ocean basins. Consequently, in our experiment the geographical extent of the particles trajectories covers the entire global ocean (see 1000 m and 2000 m Movies S1 and S2 in the supporting information). By studying the trajectories of successfully sequestered particles it becomes apparent that there is no well-defined deep advective pathway out of the SO. Instead, particle advection out of the SO is distributed relatively evenly across all longitudes, not including the western boundary currents. Figure 2 indicates the density of trajectories of particles that remained sequestered for the entire 100 year simulation. In Figure 2 the highest density of sequestered particle trajectories is within the Ross Gyre, which suggests that this location may facilitate carbon sequestration. In our model the Ross Gyre feeds Lagrangian particles into the narrow westward bound Antarctic Slope Current (ASC). Once within the ASC, particles can be entrained into Antarctic Bottom Water via deep-water formation along the slopes of the Antarctic continent [*Nicholls et al.*, 2009].

Figure 3a illustrates geographical patterns in the time taken for failed particles to be advected across MLDX, relative to their starting positions. The Weddell Gyre is a prominent feature within Figure 3a, where the time taken for particles to fail is longest in the center of the gyre, and then decreases toward its periphery. This pattern occurs because particles starting in the Weddell Gyre become trapped in its strong cyclonic motion

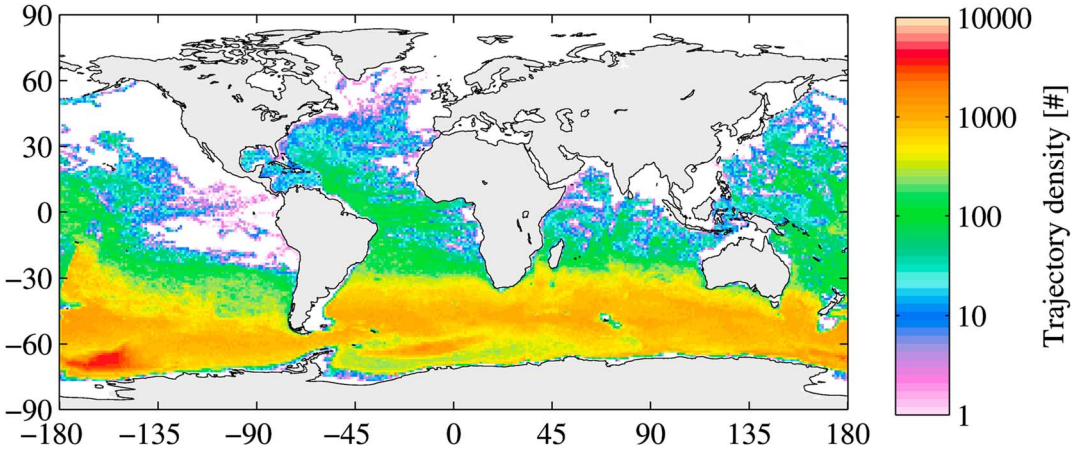

Figure 2. Time-integrated (0–100 years) census of successfully sequestered particles to illustrate their horizontal dispersal. Colors denote the cumulative "density" of particle trajectories based on monthly position throughout the simulation. Note that, for clarity, the color scale is shown in log units.

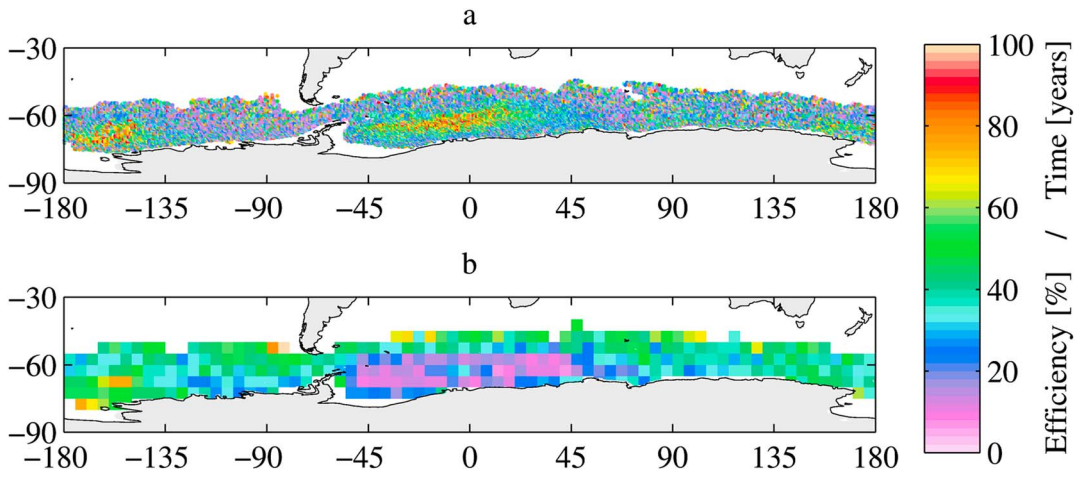

Figure 3. (a) Markers are located at the initial positions of unsuccessful Lagrangian particles at the beginning of the 100 year simulation. The color of a marker represents the time (years) at which the Lagrangian particle breached the mixed layer depth. Particles that did not upwell during the simulation are not included in the plot. (b) Efficiency of sequestration based on the criterion that a particle has to remain below the upper mixed layer to be classed as sequestered. The color of each $5° \times 5°$ grid cell represents the percentage of particles initially in that cell which remain sequestered for the entire 100 year simulation. Grid cells with fewer than 10 particles have not been included in the plot.

[*Williams and Follows*, 2011] which prolongs upwelling to an average of 55.2 years (σ = 20.8) in the core of the gyre (experiment average: 37.8 years, σ = 22.2). Of the particles that start in the Weddell Sea, 85% are advected into the UML, which is the highest failure rate of any region within the SO. The Ross Gyre is also a prominent feature in Figure 3a, though unlike the Weddell Gyre, this location may instead be suitable for OIF due to the connection with the ASC and consequent deep-water formation along the edge of the continental shelf.

Aside from the Weddell and Ross Gyres, there is little clustering within Figure 3a which suggests that particles that start next to each other in the experiment can experience radically different fates. This high sensitivity to initial conditions may be attributed to the vigorous circulation of the SO which has a number of meandering fronts particularly between the latitude bands of 60°S and 40°S [*Rintoul*, 2011].

Based on our criterion for carbon sequestration, Figure 3b shows the geographical distribution of sequestration efficiency, indicating how much sequestration results from particles seeded in each area. As in Figure 3a, the Ross Sea shows up as an area that has high rates of success, while the Weddell Sea is a mixture of areas of relatively high (center of the gyre) and low (peripheral regions) sequestration. A notable low efficiency patch in Figure 3b occurs at roughly 45°E and 60°S. Particles starting in this location become trapped in the ACC eastbound flow and consequently are lifted up and over the Kerguelen Plateau. Note that sequestration efficiency here relates to the 100 year window of our simulation, and that numerous particles ostensibly sequestered here might escape in a longer simulation.

Having studied the depth criterion (1000 m) suggested by the IPCC AR4, we conducted a sensitivity experiment that injected Lagrangian particles at a depth of 2000 m. By the end of this experiment (100 years), only 29% of the particles had breached MLDX taking an average time of 58.4 years (σ = 22.1), with 71% of the particles remaining sequestered for the entire simulation. Further analysis revealed that, of the 29% of particles that did upwell, the vast majority (98%) were again upwelled within the SO, with an average time scale of 58.3 years (σ = 22.1).

4. Discussion

The SO has been repeatedly highlighted as the best area for OIF as it is the largest HNLC region on earth, with potential for large-scale OIF leading to a noticeable impact on atmospheric CO_2 concentrations [*Lampitt et al.*, 2008]. From the paleorecord it is evident that the SO plays a key role in regulating atmospheric CO_2 content, potentially sequestrating up to 100 Pg C in the past [*Kohfeld et al.*, 2005]. Consequently, the SO has been the site of a number of iron addition experiments [*Boyd et al.*, 2012] which generally suggest that OIF does result in enhanced export at the time of fertilization.

Based on these experiments, this study assumes that OIF can enhance export of POC to depth and assesses the impact of ocean circulation on the efficiency of intentional OIF in the SO, specifically focusing on how much deep-sequestered carbon is brought back into contact with the atmosphere downstream of the fertilization site. In our 1000 m experiment, designed to trace the fate of the sequestered carbon for 100 years, 66% was upwelled into the UML on a mean time scale of 37.8 (σ = 22.2) years (Figure 2). The majority (97%) of the carbon brought back into contact with the atmosphere is upwelled within the SO, taking an average time scale of 37.4 (σ = 22.2) years. Such a "leakage" within the vicinity of the fertilization patch questions whether the SO is as good a location for OIF as initially thought.

However, even if the carbon is leaked into the UML there is no guarantee that it would be immediately outgassed. To try and assess the robustness of the fail criteria used in the analysis, the percent failed was recalculated, but allowing the particles 12 consecutive months in the UML without being classed as failed so long as they are resubducted beneath MLDX within a year. This only reduced the failure rate by 4%, which suggests that advection into the UML generally results in a long stay in the mixed layer, which greatly increases the risk of outgassing. However, if the carbon is brought back to the surface, one must assume so too is the Fe associated with it; however, this is highly dependent on the time scales of upwelling, and whether this Fe would be bioavailable for further fertilization is nontrivial [*Jiang et al.*, 2013].

Focusing on successful sequestration for 100 years in our experiment, Figure 2 illustrates the wide geographical extent of the sequestered carbon dispersed by ocean circulation. At the end of the 100 years, only 46% of the sequestered carbon initialized at 1000 m remained within the SO, with the fraction being slightly higher (56%) for the 2000 m experiment. The dispersion evident in our results demands highly sophisticated methods of observation and modeling if validation of carbon sequestration is to be carried out to an acceptable level. In any future commercialization of OIF, the fraction of the sequestered carbon which remains in the deep ocean must be properly estimated [*Rickels et al.*, 2010]. However, as Figure 2 illustrates, the global-scale dispersal of over half of the sequestered carbon presents serious logistical difficulties for monitoring. Furthermore, this dispersal may additionally interfere with attempts to attribute ownership and to allocate carbon credits appropriately (see 1000 m and 2000 m Movies S1 and S2 in the supporting information).

To date, intentional OIF has been examined in a number of modeling studies employing different criteria to quantify the efficacy of OIF (Table S3 in the supporting information), such as the overall reduction in atmospheric CO_2 by the end of the simulation [*Aumont and Bopp*, 2006] or the cumulative CO_2 uptake divided by the cumulative iron addition [*Sarmiento et al.*, 2010]. These studies have effectively assessed OIF efficiency end to end: the impact on primary production, the impact on export of POC to the deep ocean, and the downstream return of carbon to the surface ocean. Our study is unique in that it separates out the impact of ocean circulation from other biogeochemical aspects of OIF to focus solely on phase 3 of OIF and the long-term fate of carbon that has ostensibly been sequestered to depth.

A number of studies [*Aumont and Bopp*, 2006; *Oschlies et al.*, 2010; *Sarmiento et al.*, 2010] report a high proportion of the sequestered carbon being reexposed to the atmosphere over a long time scale; however, the processes or time scales in these models were not discussed. A particular advantage of our study is the use of a much higher resolution 1/4° physical model. This provides an improved representation of important fine-scale circulation features that are not present in the coarse-resolution models (2°–3°) previously employed for OIF studies (see Table S3 in the supporting information). As our study highlights the importance of the circulation in determining global efficiency of OIF, this suggests that models of even higher resolution may be required for an accurate assessment of the geoengineering potential of OIF.

In a related study, which does discuss sequestration time scales, *DeVries et al.* [2012] find a biological pump sequestration efficiency over 100 years globally of about 0.3 (i.e., 30%) [*DeVries et al.*, 2012, Figure 3c], with higher efficiency in small regions, such as the Weddell Sea—results not dissimilar to those in this paper. However, their study does not address the question of OIF explicitly and is carried out with a steady state ocean circulation model at low resolution (2°).

Figure 4 compares the 1000 m and 2000 m experiments, showing a decadal time series of the fraction of carbon remaining below the UML. Unsurprisingly, carbon exported to depths of 2000 m has a significantly higher probability of remaining sequestered for a period of 100 years than carbon exported to only 1000 m depth. As only relatively modest sequestration of carbon reaching 1000 m occurs, this would suggest

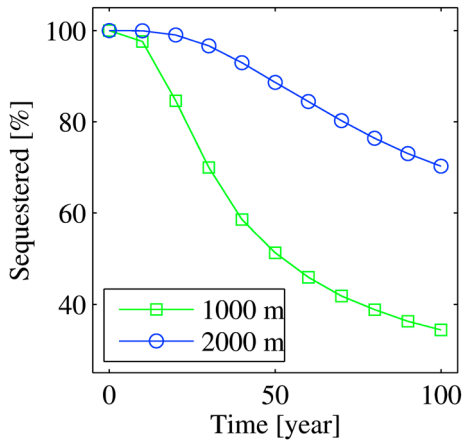

Figure 4. Decadal time series showing the number of particles that remain successfully sequestered below the upper mixed layer for both the 1000 m (green line) and 2000 m (blue line) experiments.

that 1000 m is insufficient as an ocean-wide standard for carbon sequestration and that deeper depth horizons are necessary to provide more reliable sequestration on a centennial time scale, for in the SO at least. This raises the question of how difficult is it to ensure such depth of export and sequestration. *de Baar et al.* [2008] state that below 100–250 m, particulate matter is vigorously respired and remineralized by bacteria so that on average only 1–10% of the sinking particulates reach depths below 1000 m. Using the *Martin et al.* [1987] export curve, we can estimate that of the sinking material from 100m, 14% makes it to 1000 m and 8% reaches 2000 m, which means that while more than 85% of the sinking flux is lost by 1000 m, the flux is decreased by less than a half between 1000 m and 2000 m. By choosing 2000 m as a reference depth, the 45% loss in exported material can be compensated by 40% gain in reducing advective leakage. This would increase the estimated efficiency of intentional OIF when the role of ocean circulation is taken into account. However, it is important to note that the *Martin et al.* [1987] curve is based on observations from the oligotrophic Pacific, whereas a recent experiment in a SO mesoscale eddy concluded that—in contrast—over 50% of the biomass was exported below 1000 m [*Smetacek et al.*, 2012].

There are several caveats for our work. One is that our experiments use present-day ocean circulation and do not take into account future climate change which is widely anticipated to have a significant impact on ocean circulation and mixing. The most pronounced impact on the conclusions of this study could be the effects of a warming ocean and freshening at middle to high latitudes, both of which will tend to increase vertical stratification [*Doney et al.*, 2012; *Sallée et al.*, 2013]. Within the framework of our experiments, increased stratification would potentially decrease the amount of carbon reexposed to the atmosphere and increase efficiency estimates. More generally, our work uses the ocean circulation from a single model at a single resolution. Future work involving a variety of models with varying resolutions, as well as using circulation fields from simulations that extend into perturbed projections of the 21st century ocean, may help resolve these uncertainties.

5. Conclusions

1. The export of carbon to a depth of 1000 m in the Southern Ocean does not guarantee its sequestration within the ocean for a period of 100 years.
2. More than 66% of sequestered carbon returns into contact with the atmosphere within 100 years, with a mean time scale of 37.8 years.
3. Within 100 years, carbon originally sequestered in the Southern Ocean is redistributed throughout the world ocean, with implications for monitoring.
4. The chaotic nature of Antarctic Circumpolar Current flow causes sequestered carbon initially in close proximity to be unpredictably and widely dispersed to different fates.
5. Carbon exported to 2000 m experiences lower leakage to the atmosphere (29%), suggesting that more stringent depth criteria may facilitate more accurate carbon credits systems.
6. Considering physical transport is just as critical as biogeochemical processes when evaluating the efficiency of OIF schemes.

Acknowledgments
We thank the National Environmental Research Council, part of the National capability in ocean modeling, for funding this research (NE/K500938/1). This study was carried out using the computational tool Ariane, developed by B. Blanke and N. Grima. The data presented in this study can be obtained by contacting the lead author. We are additionally grateful to a number of colleagues at NOC for suggestions and assistance, in particular A. L. New and M. Sonnewald.

The Editor thanks Michael Hiscock and an anonymous reviewer for their assistance in evaluating this paper.

References

Antonov, J. I., et al. (2010), NOAA Atlas NESDIS 69, in *World Ocean Atlas 2009, Volume 2: Salinity*, edited by S. Levitus, 184 pp., U. S. Gov. Printing Oficce, Washington, D. C.

Aumont, O., and L. Bopp (2006), Globalizing results from ocean in situ iron fertilization studies, *Global Biogeochem. Cycles*, *20*, GB2017, doi:10.1029/2005GB002591.

Blanke, B., and S. Raynaud (1997), Kinematics of the Pacific Equatorial Undercurrent: An Eulerian and Lagrangian approach from GCM results, *J. Phys. Oceanogr.*, *27*, 1038–1053.

Boyd, P. W., D. C. E. Bakker, and C. Chandler (2012), A new database to explore the findings from large-scale ocean iron enrichments experiments, *Oceanography*, *25*, 64–71, doi:10.5670/oceanog.2012.104.

de Baar, H. J. W., L. J. A. Gerringa, P. Laan, and K. R. Timmermans (2008), Efficiency of carbon removal per added iron in ocean iron fertilization, *Mar. Ecol. Prog. Ser.*, *364*, 269–282, doi:10.3354/meps07548.

DeVries, T., F. Primeau, and C. Deutsch (2012), The sequestration efficiency of the biological pump, *Geophys. Res. Lett.*, *39*, L13601, doi:10.1029/2012GL051963.

Doney, S. C., et al. (2012), Climate change impacts on marine ecosystems, *Annu. Rev. Mater. Sci.*, *4*, 11–37, doi:10.1146/annurev–marine-041911-111611.

Intergovernmental Panel on Climate Change (IPCC), Working Group I (WGI) (2007), Observations: Ocean climate change and sea level, in *Climate Change 2007: The Physical Science Basis*, edited by S. Solomon et al., pp. 385-432, Cambridge Univ. Press, Cambridge, U. K., and New York.

Intergovernmental Panel on Climate Change (IPCC), Working Group I (WGI) (2013), Summary for Policymakers, in *Climate Change 2013: The Physical Science Basis*, edited by T. F. Stocker et al., Cambridge Univ. Press, Cambridge, U. K., and New York.

Intergovernmental Panel on Climate Change (IPCC), Working Group III (WGIII) (2007), Mitigation from a cross-sectoral perspective, in *Climate Change 2007: Mitigation of Climate Change*, edited by B. Metz et al., pp. 619-690, Cambridge Univ. Press, Cambridge, U. K., and New York.

Jiang, M., et al. (2013), The role of organic ligands in iron cycling and primary productivity in the Antarctic Peninsula: A modeling study, *Deep Sea Res. Part II*, *90*, 112–133, doi:10.1016/j.dsr2.2013.01.029.

Kohfeld, K. E., C. Le Quéré, S. P. Harrison, and R. F. Anderson (2005), Role of marine biology in glacial-interglacial CO_2 cycles, *Science*, *308*, 74–77, doi:10.1126/science.1105375.

Lampitt, R. S., et al. (2008), Ocean fertilization: A potential means of geoengineering?, *Philos. Trans. R. Soc. A*, *366*, 3919–3945, doi:10.1098/rsta.2008.0139.

Leinen, M. (2008), Building relationships between sientists and business in ocean iron fertilization, *Mar. Ecol. Prog. Ser.*, *364*, 251–256, doi:10.3354/meps07546.

Locarnini, R. A., et al. (2010), NOAA Atlas NESDIS 68, in *World Ocean Atlas 2009, Volume 1: Temperature*, edited by S. Levitus, pp. 184, U. S. Gov. Printing Office, Washington, D. C.

Madec, G., (2008), NEMO reference manual, ocean dynamic component: NEMO-OPA, Notes du pole de modelisation, *Tech. Rep. 27*, Institut Pierre Simmon Laplace (IPSL), France.

Martin, J. H., G. A. Knauer, D. M. Karl, and W. W. Broenkow (1987), VERTEX: carbon cycling in the northeast Pacific, *Deep Sea Res. Part A*, *34*, 267–285.

Martin, J. M. (1990), Glacial-interglacial CO_2 change: The iron hypothesis, *Paleoceanography*, *5*, 1–13.

Monterey, G., and S. Levitus (1997), *Seasonal Variability of Mixed Layer Depth for the World Ocean. NOAA Atlas NESDIS 14*, 96, U. S. Gov. Printing Office, Washington, D. C.

Nicholls, K. W., et al. (2009), Ice-ocean processes over the continental shelf of the southern Weddell Sea, Antarctica: A review, *Rev. Geophys.*, *47*, RG3003, doi:10.1029/2007RG000250.

Oschlies, A., W. Koeve, W. Rickels, and K. Rehdanz (2010), Side effects and accounting aspects of hypothetical large-scale Southern Ocean iron fertilization, *Biogeosciences*, *7*, 4017–4035, doi:10.5194/bg-7-4017-2010.

Passow, U., and C. A. Carlson (2012), The biological pump in a high CO_2 world, *Mar. Ecol. Prog. Ser.*, *470*, 249–271, doi:10.3354/meps09985.

Popova, E. E., A. Yool, Y. Aksenov, and A. C. Coward (2013), Role of advection in Arctic Ocean lower trophic dynamics: A modeling perspective, *J. Geophys. Res. Oceans*, *118*, 1571–1586, doi:10.1002/jgrc.20126.

Rickels, W., K. Rehdanz, and A. Oschlies (2010), Methods for greenhouse gas offset accounting: A case study of ocean iron fertilization, *Ecol. Econ.*, *69*, 2495–2509, doi:10.1016/j.ecolecon.2010.07.026.

Rintoul, S. R. (2011), The Southern Ocean in the Earth System, in *Science Diplomacy: Antarctica, Science, and the Governance of International Spaces*, edited by P. A. Berkman et al., pp. 175–187, Smithsonian Institution Scholarly Press, Washington, D. C.

Sallée, J. B., E. Shuckburgh, N. Bruneau, A. J. S. Meijers, T. J. Bracegirdle, and Z. Wang (2013), Assessment of Southern Ocean mixed-layer depths in CMIP5 models: Historical bias and forcing response, *J. Geophys. Res. Oceans*, *118*, 1845–1862, doi:10.1002/jgrc.20157.

Sarmiento, J. L., and N. Gruber (2006), *Ocean Biogeochemical Dynamics*, Princeton Univ. Press, Princeton, N. J., and Oxford, U. K.

Sarmiento, J. L., et al. (2010), Efficiency of small scale carbon mitigation by patch iron fertilization, *Biogeosciences*, *7*, 3593–3624, doi:10.5194/bg-7-3593-2010.

Smetacek, V., et al. (2012), Deep carbon export from a Southern Ocean iron-fertilized diatom bloom, *Nature*, *487*, 313–319, doi:10.1038/nature11229.

Sprintall, J., and M. F. Cronin (2009), Upper Ocean Vertical Structure, in *Elements of Physical Oceanography*, edited by H. Steele, S. A. Thorpe, and K. K. Turekian, Elsevier Ltd., London, U. K.

Williams, R. G., and M. J. Follows (2011), *Ocean Dynamics and the Carbon Cycle Principles and Mechanisms*, Cambridge Univ. Press, Cambridge, U. K.